Removal of nitrate using activated carbon-based electrodes for capacitive deionization

Shaojie Jiang, Hongwu Wang, Guanquan Xiong, Xinlei Wang and Siying Tan

ABSTRACT

The removal performance of nitrate using capacitive deionization (CDI) of activated carbon (AC)-based electrodes were studied. The AC electrode was prepared and the effect of cell voltage, flow rate and initial solution concentration on ion removal were investigated. Furthermore, the AC was modified with phosphoric acid (ACP) and the surface structure of AC and ACP were analyzed. The results showed that the specific surface area of AC increased by 10.71% after the modification. The mesopore ratio and micropore ratio increased by 14.69% and 24.06%, respectively. The optimal conditions of AC electrode was a voltage of 1.4 V and flow rate of 20 mL/min while the ACP electrode was a voltage of 1.4 V and flow rate of 10 mL/min. The electrosorption capacity of ACP electrode was improved and the unit of electrosorption load was high to 19.28 mg/L. For the AC or ACP electrode, the nitrate removal efficiency decreases with the increase in the initial feed solutions, but the unit electrosorption load gradually increased with the improvement of initial feed solutions' concentration and the ACP electrode was superior to the AC electrode. Therefore, the ACP electrode would be suitable for the application of CDI on the nitrate removal.

Key words | activated carbon, desalination technology, electrosorption, phosphoric acid modification, water treatment

Shaojie Jiang (corresponding author)
Hongwu Wang
Guanquan Xiong
Xinlei Wang
Siying Tan
Key Laboratory of the Three Gorges Reservoir Region's Eco-Environment, Ministry of Education,
Chongqing University,
Chongqing 400045,
China
E-mail: *szhjzx@126.com*

INTRODUCTION

Nitrate is one of the most widespread groundwater contaminants in the world due to its high water solubility. High concentrations of NO_3^- in water poses a serious threat to human health and causes eutrophication. Recent studies had suggested that excess NO_3^- in drinking water may also be responsible for causing diverse kinds of cancers in humans (Bhatnagar & Sillanpaa 2011). Moreover, from the angle of the environment, the increase in the algae population depletes dissolved oxygen in water, increasing the risk of death in certain aquatic organisms. Therefore, the removal of nitrate from the water has attracted much attention.

The methods used for removing NO_3^- from water, including ion exchange (Samatya *et al.* 2006), biological treatment (Shrimali & Singh 2001), reverse osmosis (RO) (Perez-Gonzalez *et al.* 2012), electrodialysis (ED) (Alvarado & Chen 2014) and biological denitrification (Soares 2000). Those technologies easily remove nitrate ions, but secondary pollutants are discharged during the process of regenerating the used resins (Bae *et al.* 2002). Capacitive deionization (CDI) is an emerging water desalination technology which is based on the electrosorption of ions on porous electrodes by applying low potentials (typically below 1.5 V) (Suss *et al.* 2015). Due to its low energy consumption, non-secondary pollution and easy regeneration compared with conventional technologies, CDI has been considered as an energy-efficient and eco-friendly desalination technology.

doi: 10.2166/ws.2018.025

The materials, such as activated carbon (AC), carbon nanofibers, carbon aerogel and carbon nanotubes can be used as electrosorption electrode (Zhan *et al.* 2011; Wang *et al.* 2012; Liu *et al.* 2014; Bian *et al.* 2015). Although these materials have excellent electrosorption performance, the manufacturing process of these materials is complicated and mass production is expensive. AC has attracted a great deal of attention as one of the most common commercially available and cost-efficient carbon materials for scaling-up application (Liu *et al.* 2015). However, in order to increase the electrode specific surface area and enhance the ability to remove ions, the surface of AC was chemically modified by alkaline and acidic solutions. In this study, AC was modified with phosphoric acid (H_3PO_4) solution. The changes of surface textural and chemical properties such as specific area, pore structure and oxygen functional groups were investigated subsequently by scanning electron microscopy (SEM), N_2 adsorption–desorption and Boehm titrations to explore the relationship between the surface properties and electrosorption performance of the AC and phosphoric acid (ACP).

METHODS

Preparation of AC electrode and ACP electrode

The carbon slurry for the AC electrodes was prepared by mixing AC, conductive carbon black and PVDF solution in a certain mass ratio of 8:1:1. Subsequently, a uniform carbon slurry which contains the right amount of N-methyl pyrrolidone was produced by stirring the mixture for 8 h using a magnetic stirrer. The slurry was then cast into the foam nickel using a coating machine, for use as a current collector. The total thickness of the AC electrode was 400 μm. The cast electrode was then dried in a vacuum oven at 60 °C for six hours. The AC electrode was obtained by cutting the cast electrode into a piece 8.5 × 10 cm^2. To remove the remaining PVDF, the AC electrode was further soaked into anhydrous ethanol for 2 h and dried in a vacuum oven at 60 °C. For the purpose of chemical modification of AC surfaces, the AC was treated in 2 mol/L phosphoric acid (H_3PO_4) solutions in the water bath shaking table at 60 °C for 24 h. Then, it was dried in an oven at 120 °C. The sample was carbonized at 750 °C for 20 min in nitrogen atmosphere. After naturally cooling down to the room temperature and washed by deionized water to the neutral, the ACP materials was obtained. Then the ACP electrode was prepared by the same way above.

Desalination performance test

The desalination experiment of the CDI device was performed in a continuous flow-through system as shown in Figure 1. The initial solution was prepared by $NaNO_3$ which the concentration is 500 mg/L, and the 225 mL solution was pumped by a peristaltic pump and passed through the unit cell at a different flow rate. A given potential was applied to the cell using a potentiostat. An adsorption experiment was performed by applying a potential for 20 min and used a conductivity meter to record the electrical conductivity per minute. The relationship between conductivity and $NaNO_3$ concentration was obtained according to a calibration curve made prior to the experiment. The desalination rate was defined as follows (Wu *et al.* 2015):

$$E = \frac{C_i - C_e}{c_i} \times 100\%$$

where E is the desalination rate; c_i (mg/L) and c_e(mg/L) are the initial and final $NaNO_3$ concentration, respectively.

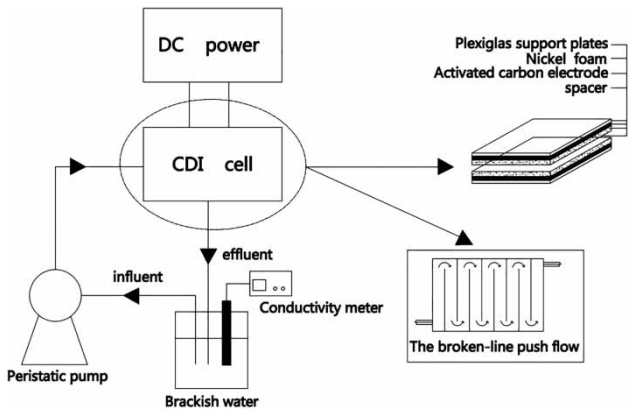

Figure 1 | Schematic representation of laboratory scale CDI unit.

RESULTS AND DISCUSSION

Characterization of the AC and ACP electrode

The morphologies of the AC and ACP electrode were observed by SEM, and SEM images of AC and ACP electrode are shown in Figure 2(a)–2(c), respectively. As shown in Figure 2(a), the ACs were well-anchored on the nickel foam substrate and showed the irregular stack structure. Figure 2(b) shows that the AC and conductive carbon black were mixed evenly under the action of PVDF, whereas some binder still remained on the surface of AC. AC electrode had a larger surface area and a porous structure on the surface. It had abundant adsorption sites. Figure 2(c) reveals the characterization of the ACP electrode. The surface of ACP was rough and showed a concave and convex shape. It suggested that the AC surface was stripped and etched, causing the collapse of the AC pore structure and forming a rough surface structure. The modification increased the surface area of AC and produced a more abundant electric adsorption sites. It enhanced the ability of electric adsorption.

Proper size and distribution of pores on the carbon electrode are significant factors affecting the electrosorption efficiency (Peng *et al.* 2011). The structural properties, including the Brunauer–Emmett–Teller (BET) surface area, total pore volume and pore size distribution (according to the BJH model), were obtained based on the N_2 adsorption–desorption isotherms, determined at 77 K using a surface area analyzer. Table 1 summarizes the BET surface areas, total pore volumes, and average pore sizes of AC and ACP for comparison. The BET surface area and total pore volume of ACP are slightly larger than AC due to the etching effect of phosphoric acid. The N_2 adsorption–desorption isotherm, as well as pore size distribution, is shown in Figure 3. For both AC and ACP, Figure 3(a) shows that the isotherm shape was somewhat transited to type IV along with the appearance of a slight hysteresis loop (H2 type) at the high pressure. This phenomenon is usually associated with the capillary condensation and suggestive of the presence of some ill-defined mesopores (Chiang *et al.* 2001). As seen from Figure 3(b), the pore volume of AC or ACP is predominantly in the pore size range <10 nm, and ACP shows a much narrower distribution of pore size and mostly concentrate around 3 nm. It indicated that the pore size distribution tended to concentrate after the modification.

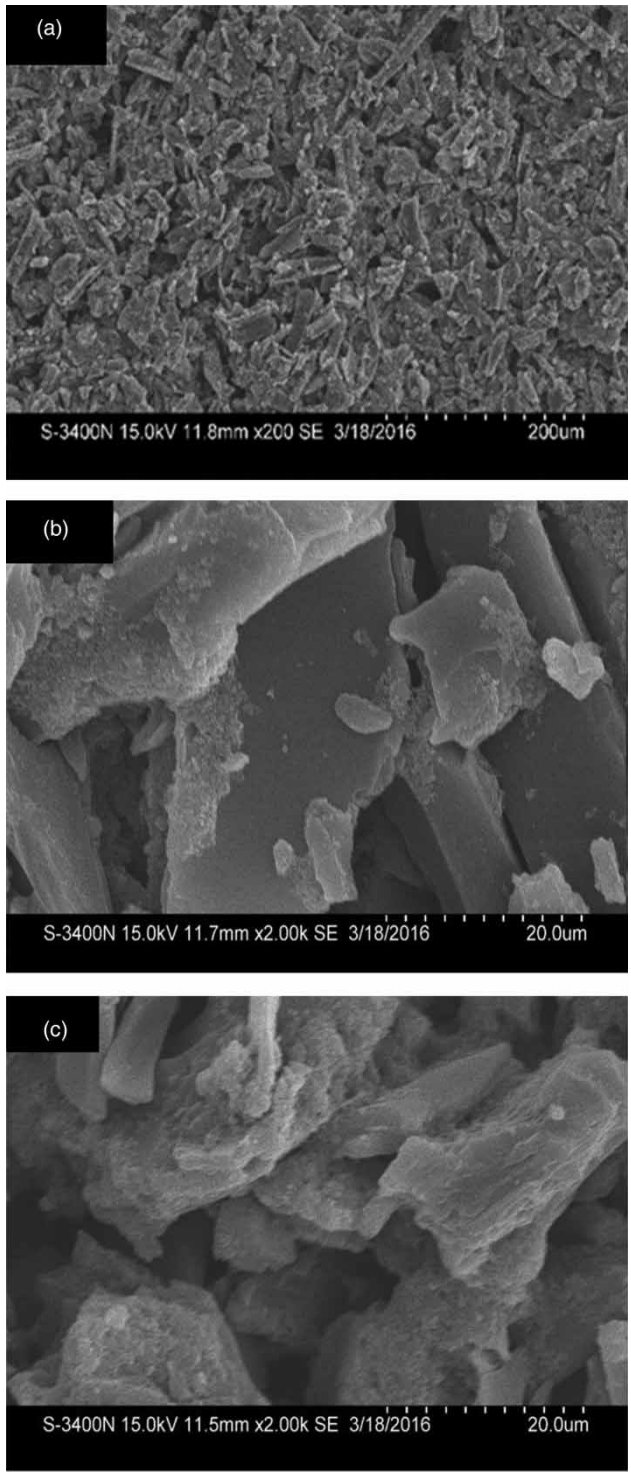

Figure 2 | SEM images of (a) and (b) AC electrode and (c) ACP electrode.

Table 1 | Brunauer–Emmett–Teller properties of AC and ACP

Sample	SBET (m^2/g)	Vtotal (cm^3/g)	Vmicro (cm^3/g)	Vmesco (cm^3/g)	Vmacro (cm^3/g)	Average pore diameter/nm
AC	1,228.15	0.9	0.187	0.667	0.046	4.533
ACP	1,359.69	1.038	0.232	0.765	0.041	4.336

Effect of the voltage on the ion removal

The applied voltage has the direct relationship with the desalination of CDI device (Han *et al.* 2013). In order to obtain the suitable voltage, the different voltages (0.8, 1.0, 1.2, 1.4, 1.6v) were applied respectively between the positive and negative electrodes for 20 min and the flow rate was kept at 20 mL/min. As seen in Figure 4(a) and 4(b), the removal rates had a fast increase before 10 min as the applied voltage rose. On the other hand, Figure 4(b) shows that the ACP electrode to remove NO_3^- increased more sharply with the potential increasing from 0.8 V to 1.6 V. It can be explained by the theoretically higher voltages inducing stronger electrostatic forces and thicker EDL, so the electrosorption capacity should increase with

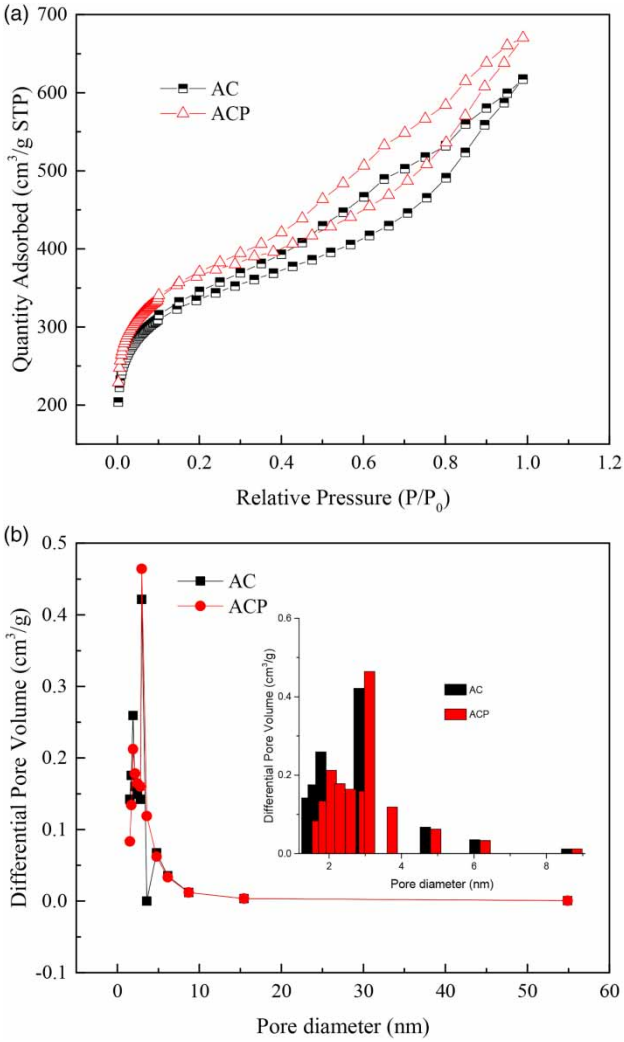

Figure 3 | (a) Nitrogen adsorption–desorption isotherms and (b) Barrett–Joyner–Halenda pore-size distribution curves for AC and ACP.

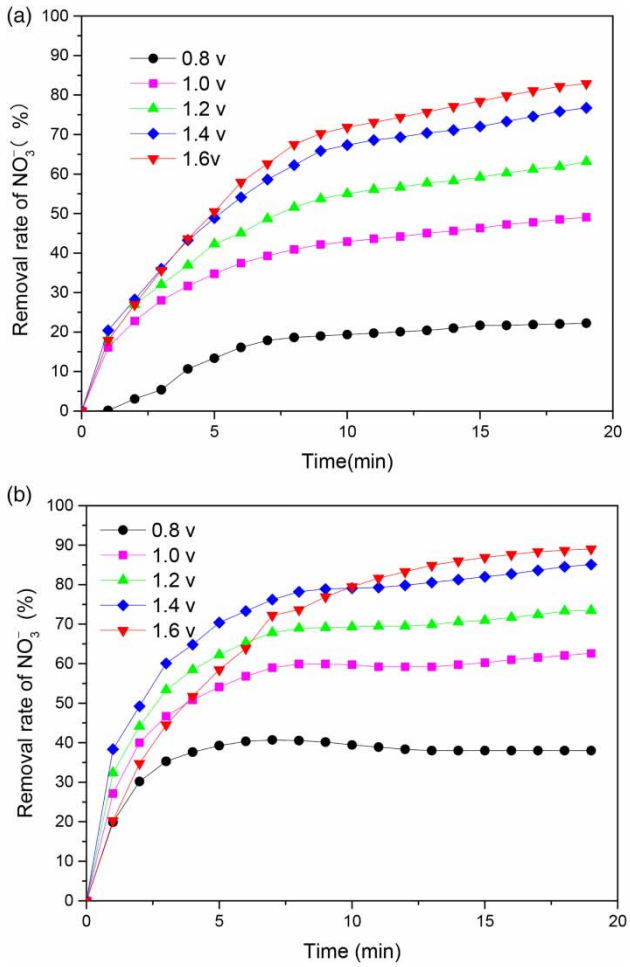

Figure 4 | The effect of operating voltage on (a) AC electrode and (b) ACP electrode.

Table 2 | The effect of voltage on the ion removal

	Voltage (V)	0.8	1	1.2	1.4	1.6
AC	Remove rate of NO_3^- (%)	22.24	49.04	63.16	76.74	82.9
ACP	Remove rate of NO_3^- (%)	37.99	62.62	73.48	85.07	89.05

the enhancement of the cell voltage. Table 2 illustrates the increase in nitrate removal from 22.24% to 82.9% for the AC electrode and the unit electrosorption load from 1.969 mg/g to 7.338 mg/g. Meanwhile, for the ACP electrode, the nitrate removal rate was increased from 37.99% to 89.05%. It proved that the modification of AC slightly accelerated the removal rate of nitrate. But when the voltage was 1.6 V, small bubbles appeared from the electrode. It suggested that the water had the electrolytic reaction which will cause the electrode corrosion (He *et al.* 2016). So the optimized value of applied potential for the AC and ACP electrode was 1.4 V.

Effect of the flow rate on the ion removal

Flow rate is also an important factor to the adsorption capacity (Mossad & Zou 2012). We studied the influence of different flow rates on the CDI by keeping the applied voltage of 1.4 V. Figure 5 shows that the electrosorption capacity improved with an increase of the flow rate up to a certain value, and then the higher the flow rate was, the lower the electrosorption capacity obtained. From Figure 5(a), the flow rate of 20 mL/min for the AC electrode was the most appropriate, because removal rate was highest. From Figure 5(b), the flow rate of 10 mL/min for the ACP electrode was the most suitable. Results displayed in Table 3 reflect that the removal rate of NO_3^- for the AC electrode was high to 76.74% under the flow rate of 20 mL/min. For the ACP electrode, the removal rate of NO_3^- was high to 92.31% under the flow rate of 10 mL/min. The faster the flow rate, the quicker the adsorption reach balance, implying much more ions adsorbed on the electrode. Nevertheless, higher flow rate can result in ions flowing away from the device, not adsorbing on the electrode in time, and the electric double layer turns thick. Inversely, lower flow rate will reduce the capacitance of desalination and increase the consumed energy and time by the same treat time (Mossad *et al.* 2013).

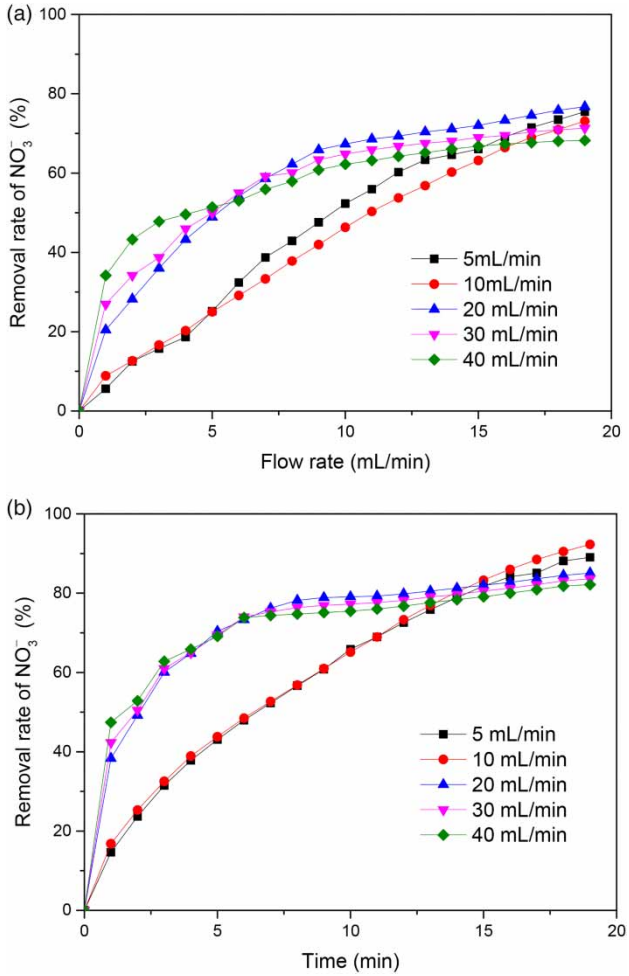

Figure 5 | The effect of flow rate on (a) AC electrode and (b) ACP electrode.

Table 3 | The effect of flow rate on the ion removal

	Flow rate (mL/min)	5.0	10.0	20.0	30.0	40.0
AC	Remove rate of NO_3^- (%)	75.47	73.12	76.74	71.31	68.23
ACP	Remove rate of NO_3^- (%)	89.05	92.31	85.07	83.62	82.17

Effect of the initial solution concentration on the ion removal

The dependence of nitrate removal efficiency and the unit electrosorption load on the initial feed solution concentrations (300, 500, 700, 900, 1,100, 1,300, 1,500, 1,700, 1,900, 2,100 mg/L) at a optimal level is shown in Figure 6. From Figure 6(a), it is clear that the nitrate removal efficiency decreases gradually with an increase in the initial

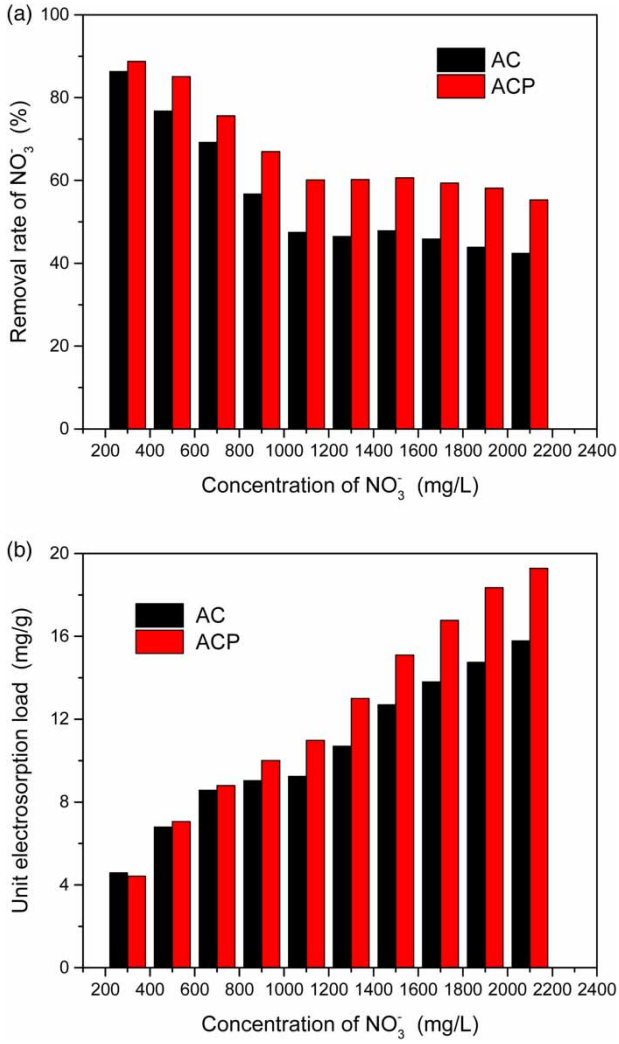

Figure 6 | The removal efficiency and the unit electrosorption load on the (a) AC electrodes at various initial feed solution at a cell voltage of 1.4 V and flow rate of 20 mL/min and (b) ACP electrodes at various initial feed solution at a cell voltage of 1.4 V and flow rate of 10 mL/min.

feed solutions. The nitrate-removal efficiency of AC electrode was 86.28% and 42.43% when using the initial feed solution values of 300 and 2,100 mg/L, respectively. The initial feed solution concentrations has little effect on the ACP electrode. It is noticed from Figure 6(b) that the increase in the initial feed solution corresponds to an initially linear increase in the unit electrosorption load on the AC and ACP electrode, which was a result of the growing diffuse double-layer capacity that depended mainly on the electrolyte solution concentration. The unit electrosorption load of ACP electrode was high to 19.28 mg/L, which is enhanced to 22.26% compared with the AC electrode. After modification by phosphoric acid, the mesopore ratio and micropore ratio increased and the active sites such as surface functional groups of the electrode could be in contact with more NO_3^- along with the increase of the initial solution concentration. Moreover, the adsorption rates and current density would be strengthened due to the decrease in the electrolyte resistance with the increase of the solution concentration (Seo *et al.* 2010). Therefore, the unit adsorption load of the ACP electrode was higher than AC electrode.

CONCLUSIONS

This study investigated the CDI performance related to removal of NO_3^- on AC-based electrodes. A modification activated carbon (ACP) with a BET-specific surface area of 1,359.69 m^2/g and some ordered mesopores (2–6 nm) that can partially avoid the EDL overlapping effect was applied for CDI experiments. We tested the effect of three main experimental parameters (cell voltage, flow rate and initial solution concentration) on NO_3^- removal during the CDI process. For the AC or ACP electrode, the nitrate removal efficiency decreased with the increase in the initial feed solutions, but the unit electrosorption load was gradually enhanced. Accordingly, the optimal level of operational parameters for AC electrode obtained by experiments included a cell voltage and flow rate of 1.4 V, 20 mL/min, respectively. For the ACP electrode, it was voltage of 1.4 V and flow rate of 10 mL/min. Under these conditions, the ACP electrodes for nitrate removal rate was 22.26% higher than the AC electrode.

REFERENCES

Alvarado, L. & Chen, A. C. 2014 Electrodeionization: principles, strategies and applications. *Electrochimica Acta* **132**, 583–597.

Bae, B. U., Jung, Y. H., Han, W. W. & Shin, H. S. 2002 Improved brine recycling during nitrate removal using ion exchange. *Water Research* **36**, 3330–3340.

Bhatnagar, A. & Sillanpaa, M. 2011 A review of emerging adsorbents for nitrate removal from water. *Chemical Engineering Journal* **168**, 493–504.

Bian, Y. H., Yang, X. F., Liang, P., Jiang, Y., Zhang, C. Y. & Huang, X. 2015 Enhanced desalination performance of membrane capacitive deionization cells by packing the flow chamber with granular activated carbon. *Water Research* **85**, 371–376.

Chiang, Y. C., Chaing, P. C. & Huang, C. P. 2001 Effects of pore structure and temperature on VOC adsorption on activated carbon. *Carbon* **39**, 523–534.

Han, L. C., Karthikeyan, K. G., Anderson, M. A., Wouters, J. J. & Gregory, K. B. 2013 Mechanistic insights into the use of oxide nanoparticles coated asymmetric electrodes for capacitive deionization. *Electrochimica Acta* **90**, 573–581.

He, D., Wong, C. E., Tang, W. W., Kovalsky, P. & Waite, T. D. 2016 Faradaic reactions in water desalination by batch-mode capacitive deionization. *Environmental Science & Technology Letters* **3**, 222–226.

Liu, Y., Nie, C. Y., Pan, L. K., Xu, X. T., Sun, Z. & Chua, D. H. C. 2014 Carbon aerogels electrode with reduced graphene oxide additive for capacitive deionization with enhanced performance. *Inorganic Chemistry Frontiers* **1**, 249–255.

Liu, D. Y., Huang, K., Xie, L. J. & Tang, H. L. 2015 Relation between operating parameters and desalination performance of capacitive deionization with activated carbon electrodes. *Environmental Science – Water Research & Technology* **1**, 516–522.

Mossad, M. & Zou, L. D. 2012 A study of the capacitive deionisation performance under various operational conditions. *Journal of Hazardous Materials* **213**, 491–497.

Mossad, M., Zhang, W. & Zou, L. 2013 Using capacitive deionisation for inland brackish groundwater desalination in a remote location. *Desalination* **308**, 154–160.

Peng, Z., Zhang, D. S., Shi, L. Y., Yan, T. T., Yuan, S. A., Li, H. R., Gao, R. H. & Fang, J. H. 2011 Comparative electroadsorption study of mesoporous carbon electrodes with various pore structures. *Journal of Physical Chemistry* **115** (34), 17068–17076.

Perez-Gonzalez, A., Urtiaga, A. M., Ibanez, R. & Ortiz, I. 2012 State of the art and review on the treatment technologies of water reverse osmosis concentrates. *Water Research* **46**, 267–283.

Samatya, S., Kabay, N., Yuksel, U., Arda, M. & Yuksel, M. 2006 Removal of nitrate from aqueous solution by nitrate selective ion exchange resins. *Reactive & Functional Polymers* **66**, 1206–1214.

Seo, S. J., Jeon, H., Lee, J. K., Kim, G. Y., Park, D., Nojima, H., Lee, J. & Moon, S. H. 2010 Investigation on removal of hardness ions by capacitive deionization (CDI) for water softening applications. *Water Research* **44**, 2267–2275.

Shrimali, M. & Singh, K. P. 2001 New methods of nitrate removal from water. *Environmental Pollution* **112**, 351–359.

Soares, M. I. M. 2000 Biological denitrification of groundwater. *Water Air and Soil Pollution* **123**, 183–193.

Suss, M. E., Porada, S., Sun, X., Biesheuvel, P. M., Yoon, J. & Presser, V. 2015 Water desalination via capacitive deionization: what is it and what can we expect from it? *Energy & Environment Science* **8**, 2296–2319.

Wang, G., Dong, Q., Ling, Z., Pan, C., Yu, C. & Qiu, J. S. 2012 Hierarchical activated carbon nanofiber webs with tuned structure fabricated by electrospinning for capacitive deionization. *Journal Materials Chemistry* **22**, 21819–21823.

Wu, T. T., Wang, G., Dong, Q., Qian, B. Q., Meng, Y. L. & Qiu, J. S. 2015 Asymmetric capacitive deionization utilizing nitric acid treated activated carbon fiber as the cathode. *Electrochimica Acta* **176**, 426–433.

Zhan, Y. K., Pan, L. K., Nie, C. Y., Li, H. B. & Sun, Z. 2011 Carbon nanotube-chitosan composite electrodes for electrochemical removal of Cu (II) ions. *Journal of Alloys and Compounds* **509**, 5667–5671.

First received 28 October 2017; accepted in revised form 18 January 2018. Available online 1 February 2018